EKSPLOATACJA I NIEZAWODNOŚĆ MAINTENANCE AND RELIABILITY

Eksploatacja i Niezawodnosc – Maintenance and Reliability

Volume 23 (2021), Issue 1

journal homepage: http://www.ein.org.pl

Article citation info:
Fan L, Wang K, Fan D. A combined universal generating function and physics of failure Reliability Prediction Method for an LED driver. Eksploatacja i Niezawodnosc – Maintenance and Reliability 2021; 23 (1): 74–83, http://dx.doi.org/10.17531/ein.2021.1.8.

A combined universal generating function and physics of failure Reliability Prediction Method for an LED driver

Indexed by: Web of Science Group

Liming Fan[a], Kunsheng Wang[a], Dongming Fan[b]*

[a]China Aerospace Academy of Systems Science and Engineering, Beijing, 100048, P. R. China
[b]School of Reliability and Systems Engineering, Beihang University, Beijing, PR China

Highlights

- The gap is bridged between the component level and the circuit system level.
- A multi-phase model is established according to function processes of circuit.
- A universal numerical approach is provided for predicting the lifetime of LED drivers.

Abstract

The accurate and effective reliability prediction of light emitting diode (LED) drivers has emerged as a key issue in LED applications. However, previous studies have mainly focused on the reliability of electrolytic capacitors or other single components while ignoring circuit topology. In this study, universal generating function (UGF) and physics of failure (PoF) are integrated to predict the reliability of LED drivers. Utilizing PoF, lifetime data for each component are obtained. A system reliability model with multi-phase is established, and system reliability can be predicted using UGF. Illustrated by a two-channel LED driver, the beneficial effects of capacitors and MOSFETs for the reliability of LED drivers is verified. This study (i) provides a universal numerical approach to predict the lifetime of LED drivers considering circuit topology, (ii) enhances the modelling and reliability evaluation of circuits, and (iii) bridges the gap between component and circuit system levels.

Keywords

reliability prediction, LED driver, reliability modelling, physics of failure, universal generating function.

Notation

$x_1,\cdots,x_n$	Independent variables in system	A	The coefficient
$u_{x_i}(z)$	Probability distribution of each variable	k	The Boltzmann constant
p_{ij}	Probability of variable i in the possible state j	E_a	The activation energy
k_{ij}	The number of states of variable x_i	T	Absolute temperature
t_A	The failure time of component A	ESR_T	The initial ESR
F_A	The cumulative distribution of component A	C	The temperature-dependent degradation rates of capacitors
$f_A(t)$	The probability density function of component A	C_0	The base degradation rate of capacitors
Q_1,Q_2	The MOSFET	A_{cap}	The surface area of the electrolytic capacitor
N_1,N_2	The windings	d	The average distance of the electrolytic capacitor
C_{1-4}	The capacity	ϖ	The conductivity of the electrolytic capacitor
LS_1,LS_2	The LED strings	RH	The relative humidity
D_1,D_2	The diodes	V_{in}	The power supply
L_{lk1},L_{lk2}	The inductors	X_{1-3}	The description of the structure in circuit

(*) Corresponding author.
E-mail addresses: L. Fan - liming_fan2020@126.com, K. Wang - kunsheng_wang@163.com, D. Fan - fdm314314@126.com

Abbreviations

SSL	Solid-State Lighting
LED	Light-Emitting Diode
LCD	Liquid Crystal Display
PF	Particle Filter
RUL	Remaining Useful Time
HCI	Hot Carrier Injection
ESR	Equivalent Series Resistance
UGF	Universal Generating Function
TTF	Time and Time to Failure
PoF	Physics of Failure

1. Introduction

As a new type of solid-state lighting (SSL), LED applications are rapidly increasing in many domains, including industrial/decorative illumination, liquid crystal display (LCD) backlighting, and automobile lamps [16] [22]. In addition to their wide range of applications, LEDs provide longer operating times and higher levels of reliability. However, compared with the lifetime of LED chips, LED drivers are found to have shorter lifetimes, as reported by the U.S. Department of Energy [33]. This discrepancy can contribute to up to 52% of total system failures [25] [29], as the operating time and reliability of LED systems are largely dependent on LED drivers [36].

In general, researchers have focused on two types of LED drivers: linear mode drivers and switch mode drivers [32] [39]. By studying LED driver schematics, many researchers have developed various approaches to predict the reliability of LED drivers. In terms of linear mode drivers, Song Lan et al. [17] presented a black box method to locate the weak point and study the reliability of a regulated LED driver circuit. A particle filter (PF) method [14] was implemented and combined with nonlinear least squares (NLS) and nonlinear mixed-effect estimation (NLME) to predict the remaining useful time (RUL). Lan et al. [15] [16] studied the degradation of a linear mode high-power LED driver, and hot carrier injection (HCI) has been revealed as the main degradation mechanism. In terms of switch mode drivers, Koosuke et al. [8] presented a diagnosis method for an output smoothing capacitor, and the lifecycle ageing rate was projected for the active circuit over the system life thanks to equivalent series resistance (ESR). Based on the PoF, Zhou [40] predicted the RUL by utilizing an accelerated ageing test.

However, several issues exist in current studies: (i) researchers have only focused on the electrolytic capacitors or other single types of components in LED drivers; (ii) the circuit topology and multiphase status of LED drivers have been ignored in previous analyses; and (iii) there has been no assurance that degradation laws and other particular factors will not change during acceleration tests. These drawbacks can lead to inaccurate prediction results, especially for complex LED driver systems with multiple phases.

To address these issues, this study aims to establish a reliability prediction model based on the operation profile of a circuit with multiple phases and bridge the gap between the component level and circuit system level. First, utilizing a PoF model, various parameters are discretized based on the failure mechanisms and the distribution model. Then, the failure probability curve can be fitted in terms of the correlation between the time and time to failure (TTF). Third, a specific two-channel switch mode LED driver is illustrated to establish the reliability model. Finally, system reliability prediction results are estimated using a UGF. The main contributions are as follows: (1) The proposed approach can provide a way to bridge the gap between the component level and circuit system level using a combined UGF and PoF approach. (2) This universal multiphase modelling approach, based on the function process of the circuit, can predict the lifetime of an LED driver.

The remainder of this paper is organized as follows. Some basic concepts, including the UGF and TTF, are introduced in Section 2. Based on the framework of the novel reliability prediction approach, the detailed modelling, analysis, and prediction of two-channel LED drivers are proposed in Section 3. The experimental procedure and results are proposed in Section 4. Finally, a discussion and conclusions are provided in Sections 5 and 6.

2. Basic conception

2.1. Universal generating function (UGF)

Generally, the reliability prediction of a circuit follows competition rules [12]. The process regards the circuit as a cascaded structure and takes the minimum lifetime of components as the lifetime. However, a competition model is clearly inaccurate in reliability prediction, especially for circuit systems with high complexity such as series-parallel and backup structures. To bridge the gap between the component level and circuit system level, the UGF approach is utilized in this paper.

The UGF approach [2] [26] [34] is typically used to describe the relationship of reliability between components and a system. It was first introduced by Ushakov [34] and generally applied in reliability assessment with multi-state components [26]. Assume that there are n independent components $x_1,\cdots,x_n$, k_i is the possible state of component x_i, and p_{ij} is the probability of component x_i at state j. The probability distribution of each variable is discretely represented by a u-function ($u_{x_i}(e^t)$) and then replaces e^t as z, as shown in (1). In an evaluation of system reliability, the u-function combines the reliability and performance to describe the component state distribution:

$$u_{x_i}(z)=\sum_{j=1}^{k_i} p_{ij}\cdot z^j \tag{1}$$

If the component is a binary unit, state 0 is the failure state, and state 1 is the success state. The u-function of component x_i can be denoted as follows:

$$u_{x_i}(z)=(1-p_i)z^0+p_i z^1 \tag{2}$$

According to a series or parallel structure, the u-function of the structure can be described as follows [2] [18]:

$$U_{series}(z)=\min\{x_1,\ldots,x_n\}=u_{x_1}(z)\underset{\times}{\otimes}u_{x_2}(z)\cdots\underset{\times}{\otimes}u_{x_n}(z) \tag{3}$$

$$U_{parallel}(z)=\max\{x_1,\ldots,x_n\}=u_{x_1}(z)\underset{\max}{\otimes}u_{x_2}(z)\cdots\underset{\max}{\otimes}u_{x_n}(z) \tag{4}$$

The reliability of the system can be described as shown in (4), in which z represents the no-fault status:

$$R=U'(z) \tag{5}$$

2.2. Time-to-failure distribution for multiple phases

An LED driver circuit has the following characteristics: (i) the circuit system can be divided into i phases based on the direction of the current and the operation of the circuit; (ii) the components have

various operation times; (iii) the TTF of components obeys various distributions; and (iv) i phases form a cycle, and the multiple cycles are serially structured [23] [35].

In accordance with the terminology introduced in [6] [7] [28], if the random variable A is in state $i(1 \le i \le n)$, or $A=i$ it simply means that A has failed in the $t_A \in [(i-1)\Delta, i\Delta]$ interval, where t_A is the failure time of component A, F_A is the cumulative distribution, Δ is the interval length $\Delta=T/n$, and n is the time granularity:

$$P(A=i) = P((i-1)\Delta < t_A \le i\Delta) = \int_{(i-1)\Delta}^{i\Delta} f_A(t)dt = F_A(i\Delta) - F_A((i-1)\Delta) \quad (6)$$

Similarly, if A is said to be in state $(n+1)$, then A has survived the mission time T:

$$P(A=n+1) = P(t_A > T) = \int_T^{\infty} f_A(t)dt = 1 - F_A(T) \quad (7)$$

3. Reliability Prediction Approach for LED Driver

3.1. Framework of reliability prediction approach

In practice, the normal degenerative process of a specific LED driver system can take years to display a conspicuous change. To address this restriction, a novel reliability prediction approach based on the PoF is proposed, which is shown in Fig. 1. Integrated with the failure mechanisms and topological structure of the system, this approach provides a universal numerical and simulation approach for predicting the lifetime of LED drivers. With the analysis of failure mechanisms, the major factors of degradation of components are determined (Step 1-Step 3). By utilizing the PoF method, the lifetime data for each component can be obtained by random sampling simulations (Step 4-Step 5). Then, the operation process of the circuit can be analysed and divided into multiple phases (Step 6). A reliability model can be established for the LED driver at each phase (Step 7). Finally, the reliability of the circuit system can be estimated with the lifetime curve above as the input data according to the topological structure of the multiphase circuit utilizing a UGF (Step 8).

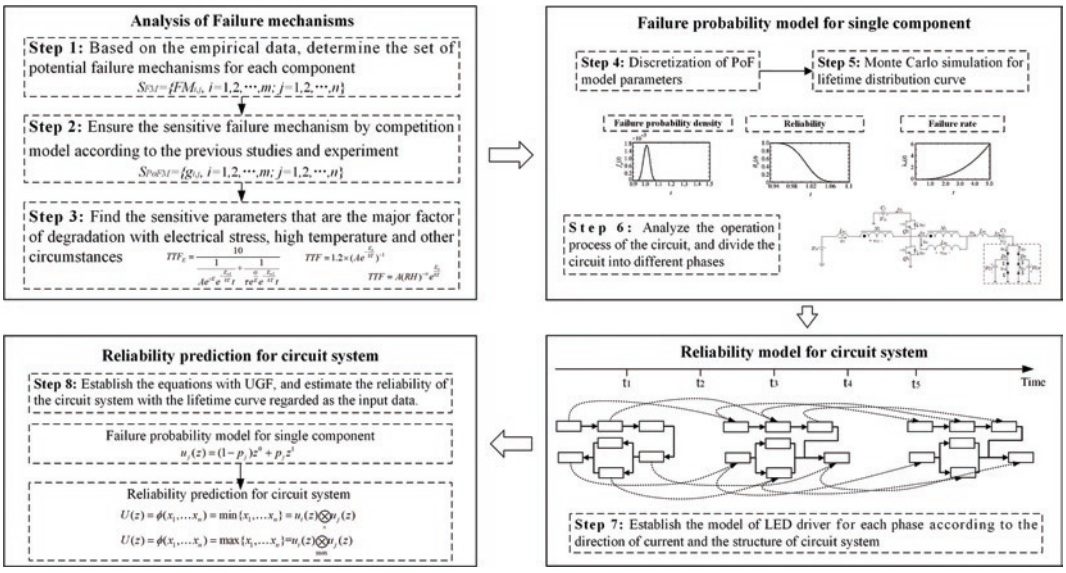

Fig. 1. The process of reliability prediction approach

3.2. Failure probability model for a single component

3.2.1. Topology of LED driver

It is well known that the balance of current is a vital function for LED drivers [32]. A switch mode LED driver has the dominant advantage in balancing the current with full bridge and half-bridge topologies. This mode features a simple structure and precise current balance. Thus, switch mode LED drivers have received increasing attention [19] [37]. Compared with the traditional topology of a switch mode LED driver, a two-channel non-isolated LED driver has the following advantages [3] [4] [9]: (i) owing to a DC-blocking capacitor, LED currents can be balanced automatically; (ii) owing to the combination of the DC-blocking capacitor and a coupled inductor, a high-output voltage gain can be achieved; (iii) the voltage spike from the leakage inductance of the coupled inductor can be recycled to the capacitor C_2 so that low-voltage MOSFETs can be used; (iv) the proposed two-channel LED driver can be extended to a multi-channel LED driver to satisfy industry requirements.

In terms of the switch mode LED driver [10] [40], a two-channel non-isolated LED driver is regarded as an example for this study, whose topology is shown in Fig. 2. It contains two MOSFETs Q_1 and Q_2, a coupled inductor composed of a primary winding N_1 and a secondary winding N_2, two energy-electrolytic capacitors C_1 and C_2, two output diodes D_1 and D_2, twooutputcapacitors C_3 and C_4, and two LED strings LS_1 and LS_2. Moreover, the coupled inductor can be modelled as an ideal transformer with a primary winding N_1 and a secondary winding N_2 connected in series with a leakage inductor L_{lk2}, a magnetizing inductor L_m connected in parallel with N_1, and a leakage inductor L_{lk1}. In addition, the current flows and the anode and cathode labels are shown in Fig. 2 [3].

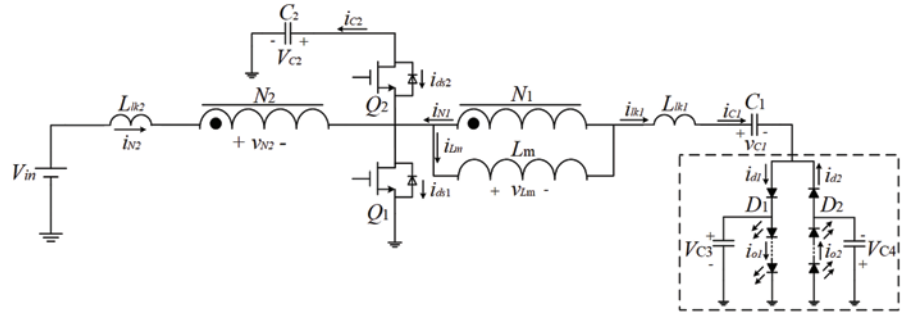

Fig. 2. The structure of the two-channel LED driver

3.2.2. PoF models

For different types of LED drivers, the topology of the circuit and component constitution are disparate, and the functional components are associated with different failure modes and mechanisms [38]. Previous reports [8] [14] [15] have discussed the failure mechanisms of amplifiers, diodes, resistors and capacitors in linear mode LED

Table 1. Mechanism models and parameter description

Component	Mechanism and formulation	Parameter description	Distribution	Feature parameter	Other parameters
MOSFET Q_1/Q_2 **[15][32][40]**	Time-dependent dielectric breakdown $TTF = (Ae^{V^m} e^{-\frac{E_a}{kT}})^{-1}$	A, E_a, k, T are the coefficient, activation energy, Boltzmann' s constant and absolute temperature, respectively; V represents voltage and m is a constant; $m = 2.9$ [40]	$A: N(\mu,\sigma)$ $T: N(\mu,\sigma)$ $V: U(a,b)$	$A: \mu$=6.98×10^{-5} $\sigma = 4.2\times10^{-6}$ $T: \mu$=328, $\sigma = 20$ $V: \mu$=0.6mV [24]	E_a=1.3eV $k = 8.62\times10^{5}$ [24]
Coupled inductor $(L_{lk1} + N_1^{'}) / (L_{lk2} + N_2)$ **[1][5]**	Corrosion $TTF = (A(RH)^{-n} e^{\frac{E_a}{kT}})^{-1}$	A is the constant related to the corrosion area; RH is the relative humidity; n is the empirical constant; E_a is the activation energy (eV); k is the Boltzmann constant (J/K); T is the absolute temperature (K)	$RH: U(a,b)$ $A: N(\mu,\sigma)$ $T: N(\mu,\sigma)$	$RH: \mu$=0.6 [5] $A: \mu$=1.785×10^{-5} $\sigma = 1\times10^{-6}$ $T: \mu$=328, σ=20	E_a=0.771eV $n = 3$ $k = 8.62\times10^{5}$ [30]
Diode [40]	Arrhenius degeneration $TTF = (Ae^{\frac{E_a}{kT}})^{-1}$	A is the coefficient; k is the Boltzmann constant (J/K); E_a is the activation energy (eV)	$A: N(\mu,\sigma)$ $T: N(\mu,\sigma)$	$A: \mu$=8.4063×10^{-5} σ=8×10^{-7} $T: \mu$=328, σ=20	E_a=1.2eV $k = 8.62\times10^{5}$ [30]
Capacitor C_1 / C_2 **[30]**	Decrease of the effective surface area $ESR(t) = ESR_T \cdot e^{C\cdot t}$ $C(t) = C_0 \cdot e^{-Ea/(k\cdot T)}$ $ESR_T = \frac{d}{A_{cap}\cdot\varpi}$	ESR_T is the initial ESR; C describes temperature-dependent degradation rates; C_0 is the base degradation rate; E_a and k are the activation energies and Boltzmann constant; A_{cap}, d, ϖ are the surface area of the electrolytic capacitor, average distance, and conductivity [40].	$C: N(\mu,\sigma)$ $T: N(\mu,\sigma)$	$C: \mu$=3.46×10^{-5} σ=2×10^{-6} $T: \mu$=328, σ=20 [30]	E_a=0.7eV $k = 8.62\times10^{5}$ [30]
Capacitor C_3 / C_4 **[31]**				$C: \mu$=3.46×10^{-5} σ=2.8×10^{-6} $T: \mu$=328, σ=20	

drivers. The reliability of a switch mode LED driver was analyzed in [30], and detailed degradation mechanisms for electrolytic capacitors, MOSFETs, inductors, diodes and sampling resistors were given.

The degradation process of a two-channel LED driver is extremely complicated and is usually caused by the gradual deterioration of components over a long period of time due to electrical stress, temperature effects, material characteristics and other circumstances. Generally, the degradation of various components can be related to specific performance parameters, and the various mechanisms can have competitive relations. Hence, according to previous research [5] [13] [20] [24] [30] [31], we focus attention on the greatest effect of each component, and the mechanism models are shown in Table 1.

To obtain the parameters of the mechanism models, the least square method is applied to fit the experimental data under various conditions. Table 1 proposes the mean values and the standard deviations, and the details of experimental data analysis, test procedures, and the fitting analysis are referred to [21].

Taking the diode as an example, we first sample the parameter based on the distribution, and the TTF data of the component can be obtained according to the number of samples. Then, we organize all the TTF data from small to large and divide the data into several groups utilizing an appropriate class. By calculating the frequency of each group, the cumulative probability can be obtained, and finally, the fitted curve between the TTF and failure probability is achieved.

In Fig. 3 (a), the x-axis represents time, and the y-axis represents the failure probability, namely, the unreliability of the component diode. The relationship between time and failure probability of the diode is shown in Fig. 3 (a). Moreover, as the various parameters of distributions change, the life curve can be different, as shown in Fig. 3 (b).

As shown in Fig. 3, the failure probability curve of the diode is proposed using the simulation method. As time goes on, the failure probability gradually increases and tends toward 1. Utilizing a temperature parameter that obeys the normal distribu-

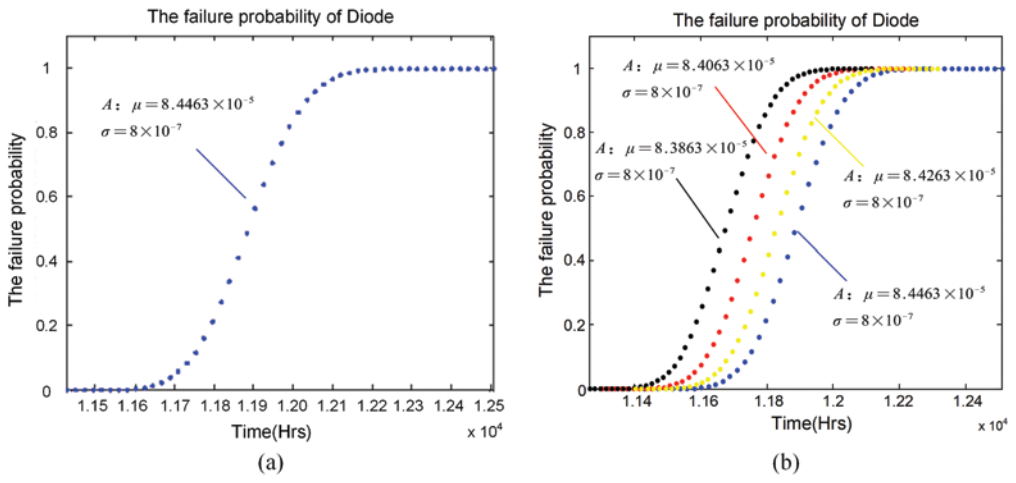

Fig. 3. The failure probability of diode: (a) failure probability curve; (b) the failure probability curve with various parameters 'A'

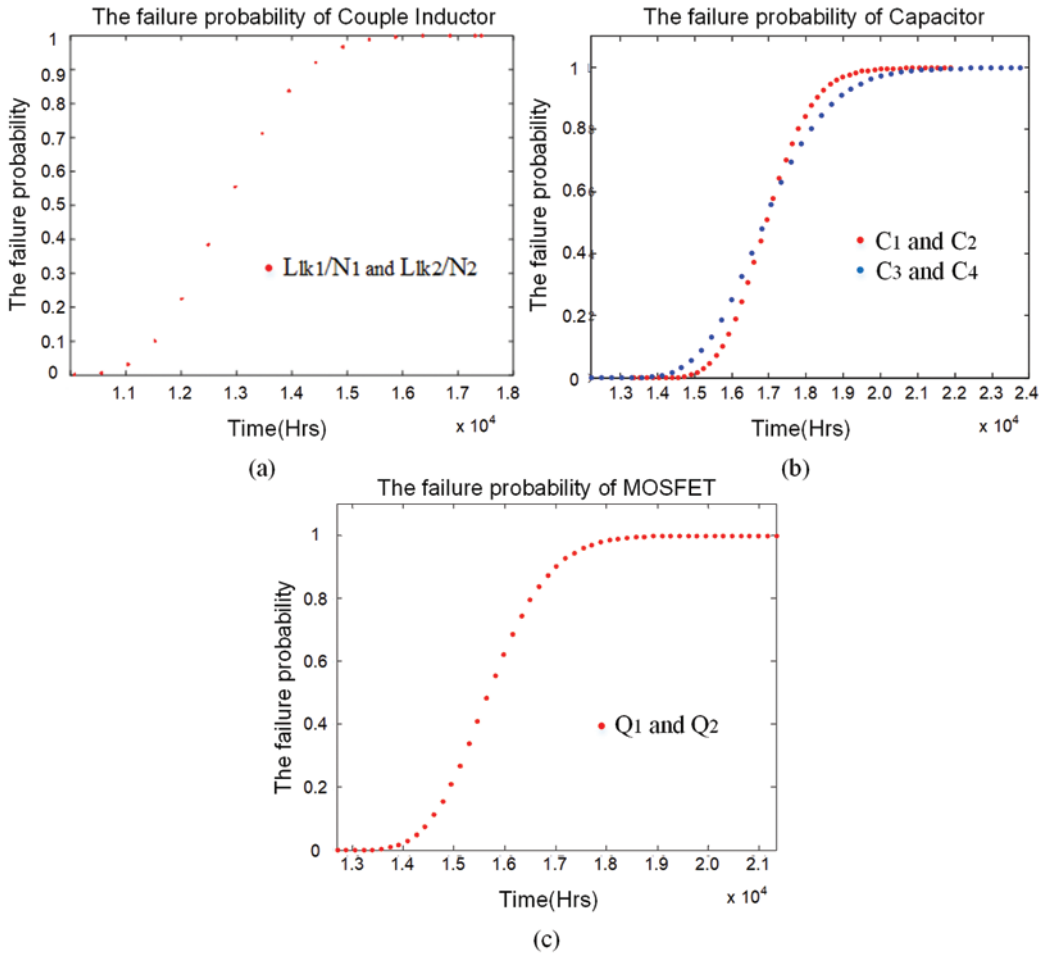

Fig. 4. The failure probability of other components: (a) the failure probability of the inductor; (b) the failure probability of the capacitor; (c) the failure probability of the MOSFET

tion, the statistical life fitting curve can be regarded as a comprehensive/general result for the components considering all the prevailing situations. Hence, the probability data at any time can be obtained based on the curve and regarded as an input prior probability to the integrated model in the next section. To simplify the analysis procedure, we assume that coupled inductors $(L_{lk1}+N_1^{'})/(L_{lk2}+N_2)$, C_1 and C_2, C_3 and C_4, Q_1 and Q_2 are the same as each other. The failure probability is shown in Fig. 4.

3.3. Reliability prediction for the two-channel LED driver

3.3.1. Modelling rules for LED driver circuit

The failure probability of the components and their corresponding lifetime curves are mentioned above. To bridge the gap between the component level and circuit system level, modelling rules and procedures are proposed [11] [27]:

(i) Define the circuit system. In this step, the scope of the system and reliability index are defined. Furthermore, its function and topology, including the components, are determined.

(ii) Determine the boundary conditions. The input, output and interface of the system are defined. Certain inductance and energy storage components can also be the input signals when they are at high potential.

(iii) Establish success criteria. Clearly define the success state and the output being focused on.

(iv) Analyze the circle process. Dismantle the operational process of the circuit based on the direction of the current.

3.3.2. Operation process of the two-channel LED driver

According to the topology structure, the operation process of the LED driver can be divided into six phases [3] [27], which are shown in Fig. 5. Switches Q_1 and Q_2 are turned on at different times, and their capacities are discharged or charged according to the electric potential. In addition, components in red represent the "OFF" state, and the "OFF" components will not deteriorate during the phase.

Model (a)-phase 1: As shown in Fig. 2 and Fig. 5 (a), Q_1 is turned ON, and Q_2 is OFF. During this state, the voltage is imposed on L_m. Meanwhile, C_1 is discharged, so i_{C1} or i_{lk1} is increasing in the opposite direction. Moreover, D_1 is reverse biased, but D_2 is forward biased. Hence, the LED string L_{S1} is supplied by C_3, whereas the LED string L_{S2} is supplied by i_{lk} in the opposite direction. This state ends when Q_1 is turned OFF [3].

Model (b)-phase 2: as shown in Fig. 2 and Fig. 5 (b), the switch Q_1 switches from ON to OFF, and the switch Q_2 still remains OFF. During this state, the voltage V_{in}-V_{C2}, which is a negative voltage, is imposed on L_{lk2} and L_m. During this blanking time, the body diode of switch Q_2 is forward biased. Because of the short time of model (b)-phase 2, we hypothesize that the body diode of switch Q_2 will have the same degeneration as switch Q_2. Moreover, D_1 is forward biased, but D_2 is reverse biased. Hence, the LED string L_{S1} is supplied by i_{lk}, whereas the LED string L_{S2} is supplied by C_4. This state ends when Q_2 is turned ON.

Model (c)-phase 3: before state 3 begins, the body diode of the switch Q_2 conducts. Thus, Q_2 is turned ON with zero-voltage switching, as shown in Fig. 2 and Fig. 5 (c), but Q_1 still remains turned OFF. In addition, the behavior of the two LED strings is the

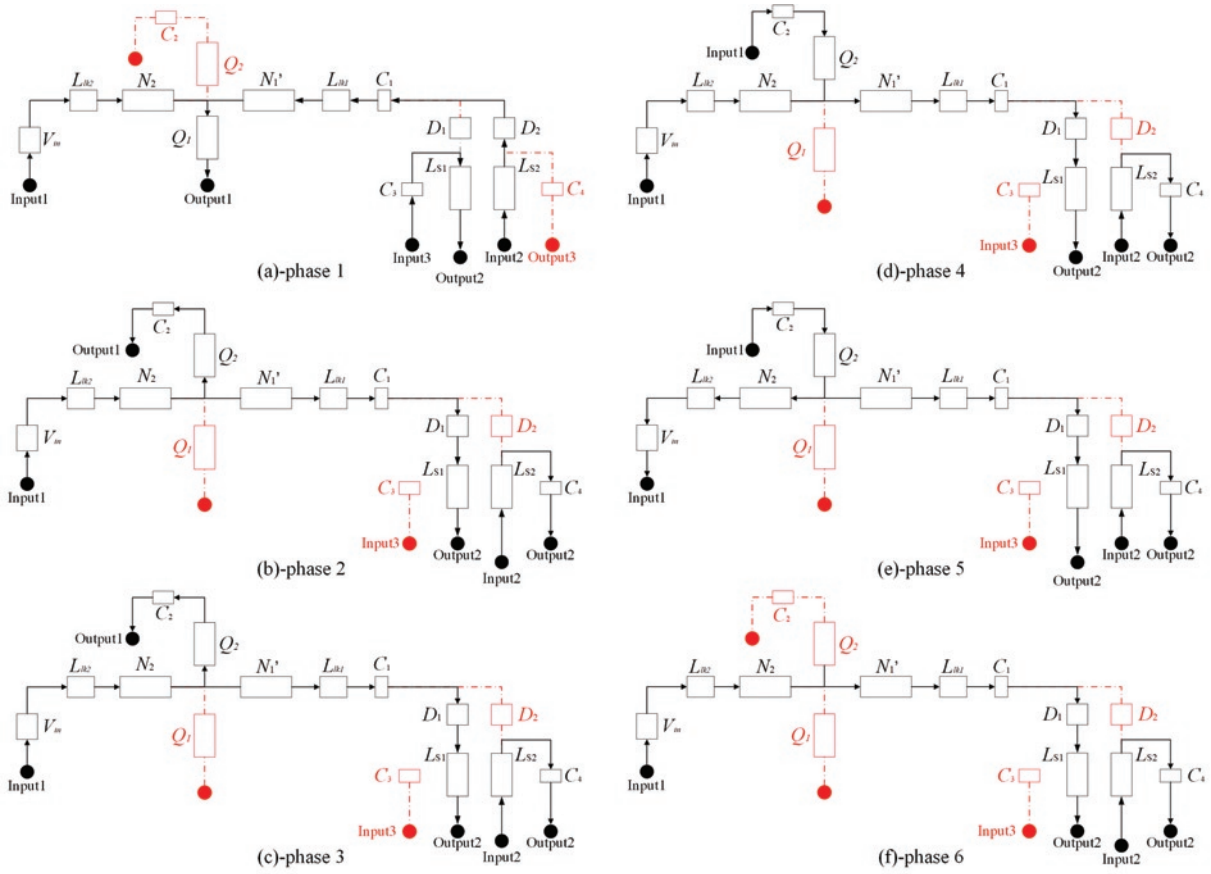

Fig. 5. The operational model of the circuit with various phases

same as that in state 2. Once i_{N2} is equal to i_{lk1}, i_{ds2} reaches zero, and this state ends.

Model (d)-phase 4: as shown in Fig. 2 and Fig. 5 (d), the switch Q_1 is still OFF, and the switch Q_2 is still ON. During this state, the capacitor C_2 is discharged, and the current i_{C2} begins to increase in the opposite direction. In addition, the behavior of the two LED strings is the same as that in model (b). This state ends when i_{N2} drops to zero.

Model (e)-phase 5: as shown in Fig. 2 and Fig. 5 (e), the switch Q_1 is still OFF, and the switch Q_2 is still ON. The direction of the current is opposite model (d)-phase 4. In addition, the behavior of the two LED strings is the same as that in model (b). This state ends when Q_2 is turned OFF.

Model (f)-phase 6: as shown in Fig. 2 and Fig. 5 (f), switch Q_1 is still OFF, and switch Q_2 turns OFF. The direction of the current is the same as model (d)-phase 4. This state ends when Q_1 is turned ON, and the next cycle is repeated.

Additionally, with the time-varying of current, the oscillations of electrical waveforms will create oscillations on the components, especially for the coupled inductors. Nonetheless, the problem oscillation is not the focus of our research, and thus, the effects on reliability are ignored in this study. This will be discussed in our future study.

3.3.3. System reliability evaluation utilizing UGF

We take model (a) as an example: the power supply V_{in} and coupled inductor (L_{lk2} and N_2) are linked as a cascade architecture, denoted by X_1; strings L_{s2}, diode D_2, capacitor C_1 and coupled inductor (L_{lk1} and equivalent N_1) are also linked as a cascade architecture, denoted by X_2. Then, X_2 is linked with coupled inductor L_{lk2}/N_2 and MOSFET Q_1 (denoted by X_4). Capacitor C_3 is in series with strings L_{s1} (denoted by X_3), as shown in Fig. 6.

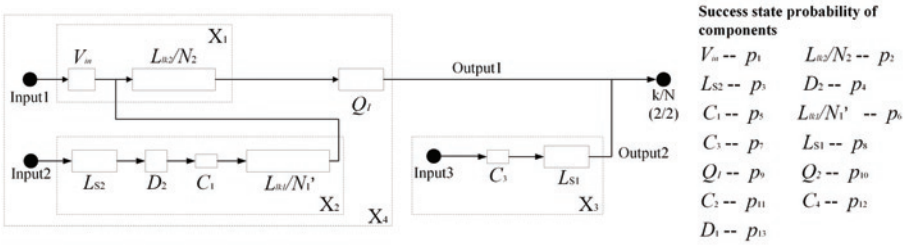

Fig. 6. The equivalent circuit of model (a)-phase 1

We assume that all the components are binary, and a logic gate of *k*-out-of-*N* is used to describe the output of the system. The structure function of the circuit can be described as follows:

$$\begin{aligned} X &= \phi(V_{in}, L_{lk2}/N_2, L_{s2}, D_2, C_1, L_{lk1}/N_1', C_3, L_{s1}, Q_1) \\ &= k/N\left\{(\min(\max(V_{in}\cdot L_{lk2}/N_2 \cdot L_{s2}\cdot D_2\cdot C_1\cdot L_{lk1}/N_1')\cdot Q_1)), (C_3\cdot L_{s1})\right\} \\ &= k/N\left\{\min((\max(X_1, X_2)\cdot Q_1)), X_3\right\} \end{aligned} \quad (8)$$

$$\begin{aligned} U_{X_1}(z) &= \left[(1-p_1)z^0 + p_1 z^1\right]\left[(1-p_2)z^0 + p_2 z^1\right] \\ &= p_{1\text{-}2}z^1 + (1-p_{1\text{-}2})z^0 \end{aligned} \quad (9)$$

$$U_{X_2}(z) = p_{3\text{-}6}z^1 + (1-p_{3\text{-}6})z^0 \quad (10)$$

$$U_{X_3}(z) = p_7 p_8 z^1 + (1-p_7 p_8)z^0 \quad (11)$$

$$U_{X_4}(z) = (p_{1\text{-}2}p_9 + p_{2\text{-}6}p_9 - p_{1\text{-}6}p_9)z^1 + (1-p_{1\text{-}2}p_9 - p_{2\text{-}6}p_9 + p_{1\text{-}6}p_9)z^0 \quad (12)$$

$$U_{X_5}(z) = U_{X_4}(z) \underset{k/N}{\otimes} U_{X_3}(z)$$
$$= (p_{1-2}p_{7-9} + p_{2-9} - p_{1-9})z^1 + (1 - p_{1-2}p_{7-9} - p_{2-9} + p_{1-9})z^0 \quad (13)$$

where $p_1 - p_{13}$ represent the probability of components in the success state, as listed in Fig. 6. The reliability of the circuit system model (a)-phase 1 in Fig. 5 can be expressed as:

$$R = U'_{X_5}(1) \quad (14)$$

Other phases in Fig. 5 can be calculated using the same process above. Focusing on analyzing the impact of component failure on the LED driver, some assumptions are made to make the analysis clear and easy. As the input of the LED driver, V_{in} has a minimal failure probability, and it can be neglected. Likewise, L_{s1} and L_{s2}, the light-emitting units that are the output of the system, are also ignored, namely, $p_1 = p_3 = p_8 = 1$. In addition, according to the failure logic of the system, the system is working properly only if all phases are in the normal state. Therefore, the various phases are regarded as a series-mode frame to evaluate the reliability of the system in this study.

According to the approach above, the reliability prediction curve for the two-channel LED driver is displayed in Fig. 7 (a). The simulation results clearly show that the reliability of the circuit gradually degrades as a function of time due to the ageing process. It also appears that the failure rate increases sharply before 18000 h and then begins to flatten gradually in Fig. 7 (b).

4. Experiments and Validation

To validate the proposed method, an experiment was designed to predict the reliability of the LED driver. The proposed type of LED drivers was selected, and 60 samples were made by Everlight Electronics, Ltd., which were used for testing. The real product is shown in Fig. 8 (a). In Fig. 8 (a), the two electrolytic capacitors are the components C_1 and C_2. The output capacitors C_3 and C_4 are parallel with light emitting diodes and thus external to the board. Owing to the necessity of the diodes to glow normally, as shown in Fig. 2, the output capacitors C_3 and C_4 should be considered in the system reliability model.

According to the sample, if the nominal constant current flowing through the LED is 350 mA, the corresponding nominal forward voltage is approximately 3.5 V. The loads of the proposed drivers were kept constant by using five 3-W white LEDs for each string. In addition, the variations in the LED forward voltage are ±10% of the nominal value, and the output power directly reflects the degradation of the LED driver, which can be conveniently measured. The main specifications of the LED driver are shown in Table 2.

Fig. 8 (b) shows the experimental setup. A local oven was used to contain the LED driver and to provide local ambient temperature control. The input voltage is controlled by the programmable power source, and the output voltage can be measured periodically by the voltage meter, thus, the state of the LED driver can be obtained. This procedure was repeated until all of the samples were in the failure state.

During the validation test, a total of 60 samples were aged individually at an ambient temperature of 328 K. With a constant input voltage, the working hours of each sample were recorded by the acceleration test until the LED driver was in a state of failure. Based on empirical data, the failure criterion is defined as within 10% of the rated current increase of the LED channel [30].

Fig. 9 shows the predicted reliability of the LED driver versus the experimental results. Due to the time limit and lab constraints, the samples are not sufficient for extensive experiments, and groups of various ambient temperatures were not considered in the experiment. Nevertheless, the prediction results are in good agreement with the

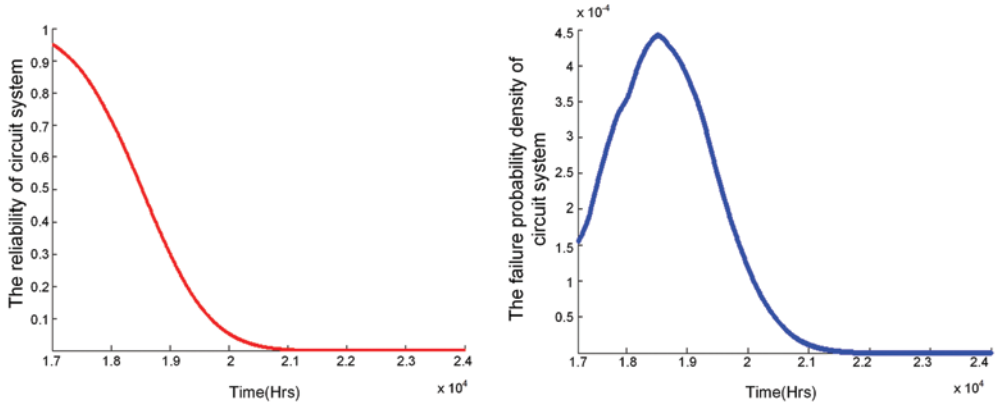

Fig. 7. Reliability prediction curve of circuit system: (a) reliability curve of system; (b) the failure probability density of system.

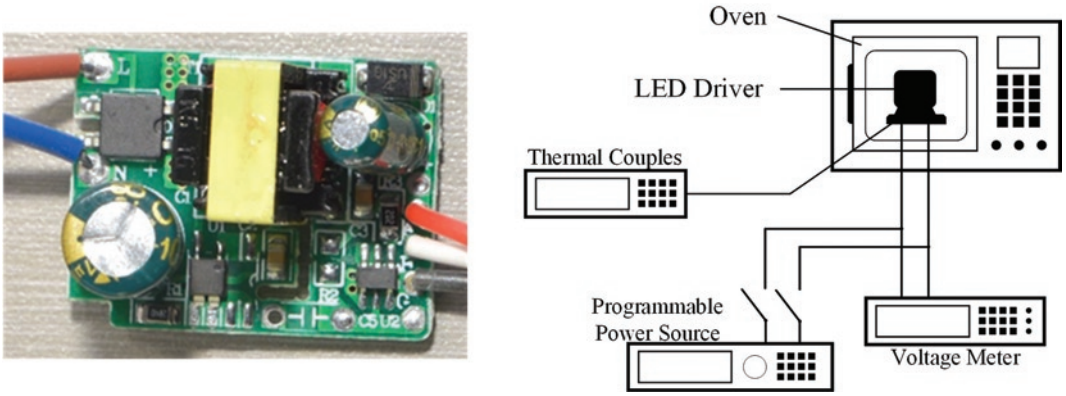

Fig. 8. (a) The layout of the specified LED driver; (b) experimental setup diagram.

Table 2. System specifications of the LED driver

System parameters	Specifications
Input voltage	$12V \pm 10\%$
Nominal LED channel voltage	$3.5V \times 5 = 17.5V \pm 10\%$
Nominal LED channel current	350 mA
Switching frequency	100 kHz

test results. The maximum error between the test and simulation is less than 10%.

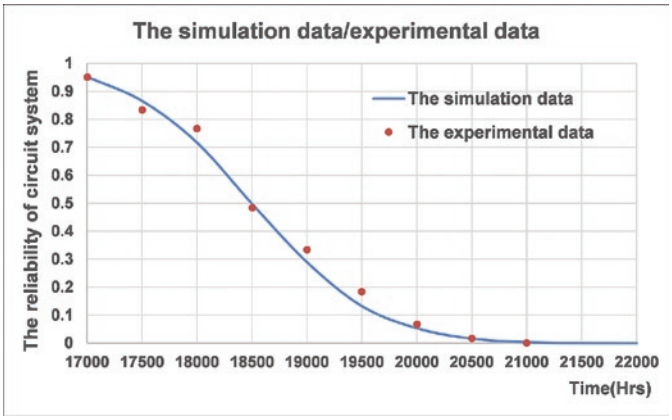

Fig. 9. Predicted reliability versus experimental data.

5. Discussions

5.1. Relevant analysis

One of the most important assumptions in modelling is that the components remain independent in the operation condition. Fig. 10 shows the reliability simulation results of the circuit system. The red line describes the degradation curve without considering the relation among the components, and the blue line displays the degradation curve with the dependence included. The results show that the reliability without considering the dependence on degrades more significantly. When the time is approximately 19500 h, the reliability that considers the relation is 0.2459, which is nearly double the value of the scenario that does not. As shown in Fig. 10, the assessment of the circuit system reliability could be more accurate with the dynamic relation between components.

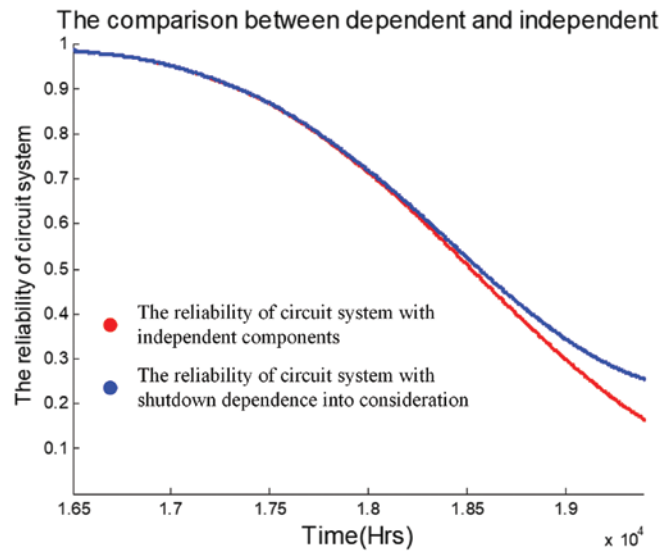

Fig. 10. Comparisons of degradation between the independent and dependent components.

5.2. Structure importance analysis of components

Fig. 11 displays the structure importance of various components. The attribute of each component to the output of the circuit system can be described quantitatively. Fig. 11 clearly shows that the higher the attribute of a component is, the greater the importance for the output of the circuit system. In Fig. 11, p_7 (C_3), p_9 (Q_1), and p_{12} (C_4) are vital components according to the entire circuit system. These components are the key objects in the structure of the circuit system.

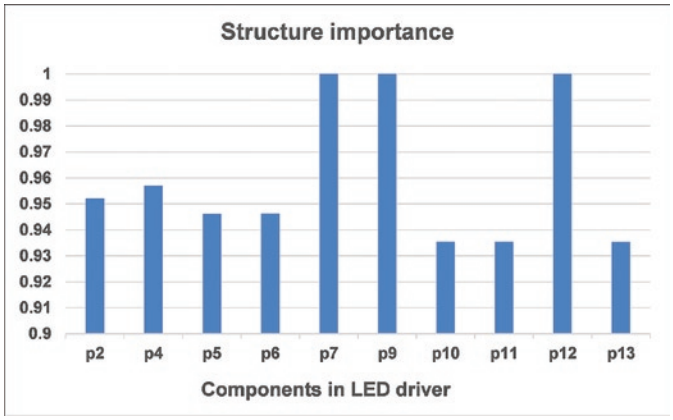

Fig. 11. The structure importance of various components

5.3. Sensitivity analysis of components

A sensitivity analysis of various components is proposed in this section. As shown in Fig. 12, p_{12} (C_4) is the most sensitive among the vital components mentioned above. This means that a slight improvement acting on the component can result in a vital effect being obtained on the LED driver. Although p_7 (C_3) and p_9 (Q_1) are vital components in the analysis of structural importance, the two components work in the first phase of the operation process. Compared with p_{12} (), the improvement of the system reliability is nearly the same, as shown in Fig. 12.

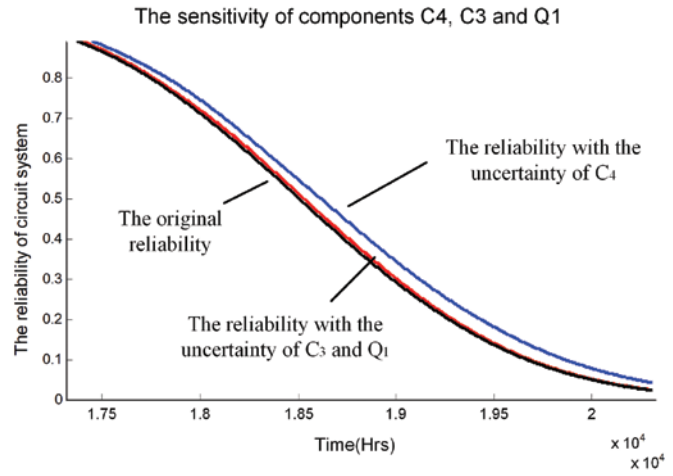

Fig. 12. Sensitivity analysis of components.

5.4. Sensitivity analysis of temperature

Fig. 13 shows the reliability sensitivity of the system to the temperature of components within a given ambient temperature. Owing to the time-varying thermal fields, the temperature of the components is unknown and uncertain. The system reliability is simulated in this study under various component temperatures (308 K, 328 K and 348 K). As shown in Fig. 13, the simulation of system reliability under 328 K is proposed, and the data with 308 K and 348 K are proposed in Fig. 13. Based on the various temperatures of the components, the failure probabilities of the system are 0.942 (348 K), 0.868 (328 K) and 0.753 (308 K) at 19500 h.

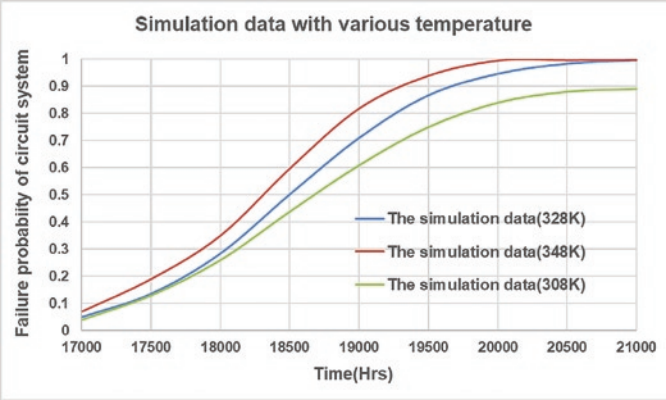

Fig. 13. Sensitivity of temperature for components

6. Conclusion

This paper proposed a graphical modelled aggregation approach to estimate the reliability and predict the lifetime of two-channel LED drivers. With the basis of the PoF of all the components in the circuit system, the simulation curves of the lifetimes for components could be obtained. Bridging the gap between the component level and circuit system level, the circuit was mapped into a reliability model according to the operation process of the circuit and based on the modelling rules. Integrated with the UGF, the reliability and lifetime prediction of LED drivers can be obtained using a formalized algorithm. This study offers the following contributions: (i) the multiphase modelling of the circuit and the quantitative calculation are enhanced by the reliability model and the UGF; (ii) the gap is bridged between the component level and the circuit system level; and (iii) a universal numerical and emulation approach is provided for predicting the lifetime of LED drivers. The following conclusions are based on the above algorithm:

(i) The reliability of the circuit gradually degrades as a function of time, and the failure rate increases sharply before 18000 h and then begins to flatten gradually.

(ii) The reliability with independent components will degrade more significantly, at nearly double the reliability of the dependent components at approximately 19500 h.

(iii) The capacitors and MOSFETs are identified as vital components of the circuit structure. Component is the most sensitive component.

The approach proposed in this study provides a universal approach, and it is applicable for all types of LED drivers that have the characteristics of multiphase and complex topological structures. However, a few open issues remain, such as the accuracy and precision of the fitting interval and the multiple states of components, which are to be studied in future work. For example, the failure analysis should confirm whether the failure modes used in the prediction approach are the same as the observed failure modes. The interconnection and multi-physical field coupling among various failure mechanisms are the main points of further research. Additionally, the effect of the operation process on practical circuits should be considered, such as the various internal and ambient temperatures, and oscillations on components remain challenging issues in the reliability prediction of LED drivers. Furthermore, the approach should also be extended to fault diagnosis by using the authentic data of the components.

References

1. Alonso JM, Viña J, Vaquero DG, MartíNez G. Analysis and design of the integrated double buck-boost converter as a high-power-factor driver for power-LED lamps. IEEE Transactions on Power Electronics 2012; 59(4): 1689-1697, https://doi.org/10.1109/TIE.2011.2109342.
2. Bao ML, Ding Y, Singh C, Shao CZ. A multi-state model for reliability assessment of integrated gas and power systems utilizing universal generating function techniques. IEEE Transactions on Smart Grid 2019; 10(6): 6271-6283, https://doi.org/10.1109/TSG.2019.2900796.
3. Chen XB, Huang DC, Li Q, Lee FC. Multichannel LED driver with CLL resonant converter. IEEE Transactions on Power Electronics 2015; 3(3): 589-598, https://doi.org/10.1109/JESTPE.2015.2417219.
4. Chen Y, Nan YR, Kong QG. A loss-adaptive self-oscillating buck converter for LED driving. IEEE Transactions on Power Electronics 2012; 27(10): 4321-4329, https://doi.org/10.1109/TPEL.2012.2190755.
5. Cirmirakis D, Demosthenous A, Saeidi N, Donaldson N. Humidity-to-frequency sensor in CMOS technology with wireless readout. IEEE Sensors Journal 2013; 13(3): 900-908, https://doi.org/10.1109/JSEN.2012.2217376.
6. Fan D, Wang Z, Liu L, Ren Y. A modified GO-FLOW methodology with common cause failure based on discrete time bayesian network. Nuclear Engineering & Design 2016; 305: 476-488, https://doi.org/10.1016/j.nucengdes.2016.06.010.
7. Feng Q, Zhao XJ, Fan DM, Cai BP, Liu YQ, Ren Y. Resilience design method based on meta-structure: A case study of offshore wind farm. Reliability Engineering & System Safety 2019; 186: 232-244, https://doi.org/10.1016/j.ress.2019.02.024.
8. Harada K, Katsuki A, Fujiwara M. Use of ESR for deterioration diagnosis of electrolytic capacitor. IEEE Transactions on Power Electronics 1993; 8(4): 355-361, https://doi.org/10.1109/63.261004.
9. Hwu KI, Jiang WZ. Expandable two-channel LED driver with galvanic isolation and automatic current balance. IET Power Electronics 2018; 11(5): 825-833, https://doi.org/10.1049/iet-pel.2017.0508.
10. Hwu KI, Jiang WZ. Non-isolated two-channel LED driver with automatic current balance and zero-voltage switching. IEEE Transactions on Power Electronics 2016; 31(12): 8359-8370, https://doi.org/10.1109/TPEL.2016.2515088.
11. Kasprzyk L. Modelling and analysis of dynamic states of the lead-acid batteries in electric vehicles. Eksploatacja i Niezawodnosc – Maintenance and Reliability 2017; 19 (2): 229–236, http://dx.doi.org/10.17531/ein.2017.2.10.
12. Kozłowski E, Mazurkiewicz D, Żabiński T, Prucnal S, Sęp J. Assessment model of cutting tool condition for real-time supervision system. Eksploatacja i Niezawodnosc - Maintenance and Reliability 2019; 21(4): 679-685, https://doi.org/10.17531/ein.2019.4.18.
13. Kozłowski E, Mazurkiewicz D, Żabiński T, Prucnal S, Sęp J. Machining sensor data management for operation-level predictive model. Expert Systems with Applications 2020; 159: 1-22, https://doi.org/10.1016/j.eswa.2020.113600.

14. Lan S, Tan CM. Application of particle filter technique for lifetime determination of a LED driver. IEEE Transactions on Power Electronics 2015; 15(2): 163-172, https://doi.org/10.1109/TDMR.2015.2407410.
15. Lan S, Tan CM. Degradation model of a linear-mode LED driver and its application in lifetime prediction. IEEE Transactions Device Mater. Reliability 2014; 14(3): 904-913, https://doi.org/10.1109/TDMR.2014.2343253.
16. Lan S, Tan CM, Wu K. Methodology of reliability enhancement for high power LED driver. Microelectronics Reliability 2014; 54(6-7): 1150-1159, https://doi.org/10.1016/j.microrel.2014.01.027.
17. Lan S, Tan CM, Wu K. Reliability study of LED driver-a case study of black box testing. Microelectronics Reliability 2012; 52(9-10): 1940-1944, https://doi.org/10.1016/j.microrel.2012.06.023.
18. Levitin G, Xing L, Dai Y. Minimum mission cost cold-standby sequencing in non-repairable multi-phase systems. IEEE Transactions on Reliability 2014; 63(1): 251-258, https://doi.org/10.1109/TR.2014.2299192.
19. Liu HW, Guo K, Zhang ZY. High-power LED photoelectrothermal analysis based on backpropagation artificial neural networks. IEEE Transactions on Electron Devices 2017; 65(7): 2867-2873, https://doi.org/10.1109/TED.2017.2701346.
20. Liu D, Wang SP, Tomovic MM. Degradation modeling method for rotary lip seal based on failure mechanism analysis and stochastic process. Eksploatacja i Niezawodnosc - Maintenance and Reliability 2020; 22(3):381-390, https://doi.org/10.17531/ein.2020.3.1.
21. Lin RL, Liu SY, Lee CC, Chang YC. Taylor-series-expression-based equivalent circuit models of LED for analysis of LED driver system. IEEE Transactions on Industry Applications 2013; 49(4): 1854-1862, https://doi.org/10.1109/TIA.2013.2258313.
22. Li SN, Tan SC, Lee CK, Waffenschmidt E, Hui R, Tse CK. A survey, classification, and critical review of light-emitting diode drivers. IEEE Transactions on Power Electronics 2016; 31(2): 1503-1516, https://doi.org/10.1109/TPEL.2015.2417563.
23. Li ZF, Wang ZL, Ren Y, Yang DZ, Lv X. A novel reliability estimation method of multi-state based on structure learning algorithm. Eksploatacja i Niezawodnosc - Maintenance and Reliability 2020; 22(1): 170-178, https://doi.org/10.17531/ein.2020.1.20.
24. Marioli D, Sardini E, Serpelloni M. An inductive telemetric measurement system for humidity sensing. Measurement Science & Technology 2008; 19(11): 1054-1057, https://doi.org/10.1088/0957-0233/19/11/115204.
25. Meneghini M, Lago MD, Trivellin N, Meneghesso G, Zanoni E. Degradation mechanisms of high-power LEDs for lighting applications: an overview. IEEE Transactions on Industry Applications 2014; 50(1): 78-85, https://doi.org/10.1109/TIA.2013.2268049.
26. Ren Y, Fan DM, Feng Q, Wang ZL, Sun B, Yang DZ. Agent-based restoration approach for reliability with load balancing on smart grids. Applied Energy 2019; 249: 46-57, https://doi.org/10.1016/j.apenergy.2019.04.119.
27. Ren Y, Fan DM, Ma XR, Wang ZL, Feng Q, Yang DZ. A GO-FLOW and Dynamic Bayesian Network Combination Approach for Reliability Evaluation with Uncertainty: A Case Study on a Nuclear Power Plant. IEEE Access 2017; 6: 7177-7189, https://doi.org/10.1109/ACCESS.2017.2775743.
28. Ren Y, Fan DM, Wang ZL, Yang DZ, Feng Q, Sun B, Liu LL. System Dynamic Behavior Modeling Based on Extended GO Methodology. IEEE Access 2018; 6: 22513-22523, https://doi.org/10.1109/ACCESS.2018.2816165.
29. Sun B, Fan XJ, Li L, Ye HY, Van DW, Zhang GQ. A reliability prediction for integrated LED lamp with electrolytic capacitor-free driver. IEEE Transactions on Components Packaging and Manufacturing Technology 2017; 7(7): 1081-1088, https://doi.org/10.1109/TCPMT.2017.2698468.
30. Sun B, Fan X, Qian X, Zhang G. PoF-simulation-assisted reliability prediction for electrolytic capacitor in LED drivers. IEEE Transactions on Industrial Electronics 2016; 63(11): 6726-6735, https://doi.org/10.1109/TIE.2016.2581156.
31. Sun B, Fan XJ, Van DM, Cui CQ, Zhang GQ. A stochastic process based reliability prediction method for LED driver. Reliability Engineering & System Safety 2018; 178: 140-146, https://doi.org/10.1016/j.ress.2018.06.001.
32. Sun B, Jiang XP, Yung KC, Fan JJ, Pecht MG. A review of prognostics techniques for high-power white LEDs. IEEE Transactions on Power Electronics 2017; 32(8): 6338-6362, https://doi.org/10.1109/TPEL.2016.2618422.
33. U.S. Department of Energy (DOE). LED luminaire lifetime: Recommendations for testing and reporting," 3rd ed. 2014. [Online]. Available: http://energy.gov/eere/ssl/led-lighting-facts
34. Ushakov IA. Universal generating function. Soviet Journal of Computer and Systems Sciences 1986; 24(5):118-129.
35. Więcławski K, Mącza J, Szczurowski K. Electric current as a source of information about control parameters of indirect injection fuel injector. Eksploatacja i Niezawodnosc - Maintenance and Reliability 2020; 22(3): 449-454, https://doi.org/10.17531/ein.2020.3.7.
36. Williams RK, Darwish MN, Blanchard RA, Siemieniec R, Rutter P, Kawaguchi Y. The trench power MOSFET-Part II: application specific VDMOS, LDMOS, packaging, and reliability. IEEE Transactions on Electron Devices 2017; 63(3): 692-712, https://doi.org/10.1109/TED.2017.2655149.
37. Wu H, Wong SC, Tse CK, Chen QH. A PFC single-coupled-inductor multiple-output LED driver without electrolytic capacitor. IEEE Transactions on Power Electronics 2019; 34(2): 1709-1725, https://doi.org/10.1109/TPEL.2018.2829203.
38. Xia Q, Yang DZ, Wang ZL, Ren Y, Sun B, Feng Q, Qian C. Multiphysical modeling for life analysis of lithium-ion battery pack in electric vehicles. Renewable & Sustainable Energy Reviews 2020; 131, https://doi.org/10.1016/j.rser.2020.109993.
39. Yadlapalli RT, Narasipuram RP, Kotapati A. An overview of energy efficient solid state LED driver topologies. International Journal of Energy Research 2020; 44(2): 612-630, https://doi.org/10.1002/er.4924.
40. Zhang H. A viable nontesting method to predict the lifetime of LED drivers. IEEE Journal of Emerging and Selected Topics in Power Electronics 2018; 6(3): 1246-1251, https://doi.org/10.1109/JESTPE.2018.2826364.
41. Zhang J, Wang J, Wu X. A Capacitor-isolated LED driver with inherent current balance capability. IEEE Transactions on Power Electronics 2012; 59(4): 1708-1716, https://doi.org/10.1109/TIE.2011.2138111.